Life Science Journal

Websites:
http://www.lifesciencesite.com
http://www.sciencepub.net

Emails:
editor@sciencepub.net
sciencepub@gmail.com

MARSLAND PRESS
Multidisciplinary Academic Journal Publisher

Effect of ozone on submandibular salivary gland of alloxan-induced diabetic rats: Histological and ultrastructural study

Doaa A. Taiema[1], Reda Gaber Saleh[2], Elsayed Mohamed Deraz[3]

[1] Lecturer of Oral Biology Faculty of Dentistry, Tanta University, Egypt
[2] Lecturer of Oral Biology Faculty of Dentistry, Tanta University, Egypt.
[3] Assistant Professor of Oral pathology, Faculty of Dentistry, Tanta University, Egypt.
E-mails: dodofirstmolar@gmail.com, redag2000@gmail.com, elsayedderaz@yahoo.com

Abstract: Background: Diabetes mellitus is a metabolic disease that is characterized by hyperglycemia resulting from insufficiency and /or dysfunction of insulin. Several pathological changes in acini and ducts of submandibular salivary gland were demonstrated in diabetes Recently, ozone has been introduced in medical filed as new therapeutic agent using its benefits effects on subsiding the destructive effects of diabetes mellitus. **Aim of study:** The current study was performed to examine the effect of ozone on submandibular salivary gland of alloxan-induced diabetic rats at histological and ultrastructural levels. **Methods:** Thirty male albino rats were randomly divided into 3 groups each one ten rats as follows; group I (control), group II (diabetic) exposed to diabetes induction model by alloxan. group III (ozone) rats received intraperitoneal administration of ozone at a dose of 1.1 mg/kg. The rats from each group were euthanized 6 weeks after experiment. The submandibular salivary glands were removed and examined at histologically and ultrastructural levels. **Results:** histological examination of diabetic rats revealed sever degenerative changes of the glandular tissue including intracytoplasmic vacuolization, different sizes and shape of the acinar cells. Atrophic striated ducts and granular convoluted tubules with retained eosinophilic secretory material. In ozone treated rats, reversion of the destructive effects of diabetes was noticed and the gland nearly exhibited a normal architecture pattern, including normal acini, striated ducts and granular convoluted tubules structure with small number of intracytoplasmic vacuolization and little amount of eosinophilic material. The ultrastructure examination of diabetic rats revealed irregular dark nuclei perinuclear spaces, large cytoplasm vacuoles, irregular dilated degenerated rough endoplasmic reticula with degenerated mitochondria in acinar cells and striated duct. Depletion of secretory vesicles in serous cells and coalescing of electron lucent secretory vesicles in mucous cells. Myoepithelial cell showed clumping of the nuclear chromatin. For ozone treated rats, glandular tissue (serous and mucous cells, striated duct) showed mostly normal structure with little signs of degenerative changes including small cytoplasm vacuoles, little amount of rough endoplasmic reticula dilatation. Myoepithelial cells appeared with normal nucleus others showed little amount of nuclear clumping chromatin. **Conclusion:** Ozone as a potent oxidizer that has a potential therapeutic role in reversing the destructive effects of diabetes on submandibular salivary gland.

[Doaa A. Taiema, Reda Gaber Saleh, Elsayed Mohamed Deraz. **Effect of ozone on submandibular salivary gland of alloxan-induced diabetic rats: Histological and ultrastructural study.** *Life Sci J* 2019;16(10):112-121]. ISSN: 1097-8135 (Print) / ISSN: 2372-613X (Online). http://www.lifesciencesite.com. 13. doi:10.7537/marslsj161019.13.

Key words: Alloxan, diabetes mellitus, histological, ozone, rat, submandibular salivary gland, ultrastructural

1. Introduction

Diabetes mellitus (DM) is a metabolic diseases characterized by hyperglycemia rising from the changed insulin secretion, insulin action, or both (1). Chronic hyperglycemia of DM is associated with long-term damage, dysfunction and organ failure as eyes, kidneys, nerves, heart and blood vessels (2). Continued hyperglycemia leads to oxidative stress, alterations in enzyme activity, protein glycosylation and numerous structural changes (3). Oral health drawbacks related with diabetes include xerostomia, gingivitis, tooth loss, and soft tissue lesions of the tongue and oral mucosa (4).

Continued Diabetes hyperglycemia causes increased generation of free radicals chiefly reactive oxygen species owing to glucose auto-oxidation and protein glycosylation which results in diabetes-induced "oxidative stress" (5). OS and its cytopathological consequences have been involved in the pathology of periodontitis, oral cancer as well as in the changes of the salivary glands function in the sequence of the diseases (6).

Besides, the salivary flow reduction can proceed in clinical dry mouth, which troubles diabetic patients. Diabetic signs are accompanied by evident morphological alterations of salivary glands, usually

described as sialadenosis(7). Studies on human submandibular salivary gland (SMG) stated alterations in gross features such as parenchymal atrophy and increased fibrous tissue, which fall within the context of sialadenosis(8).

Ozone is an unstable gas quickly giving up immature oxygen that is a strong oxidant rendering multiple useful effects like an effective antimicrobial agent, metabolic & immune modulation, interruption of tumor metabolism, sterilization of medical & dental equipment, purification of drinking water etc(9).

The therapeutic effects of ozone therapy were studied in streptozotocin (STZ)-induced diabetic rats(10). Treatment with either insulin or ozone therapy significantly reversed the effects of DM (11).

In the literature there are few ultrastructural reports regarding the effect of ozone on SMG in diabetes. Therefore, the aim of the present investigation was to examine the effect of ozone on SMGs of rats with alloxan-induced diabetes at histological and ultrastructural levels.

2. Materials and Methods

Animals

Albino male rats (200-230g) were selected. The animals were served in animal house of Histology Department, Faculty of Medicine, Tanta University. The rats were kept on a 12 day night / dark at (22 ± 2°C, 55%- 70% humidity). They received a diet of standardized pellets and free acess to tap water. We have followed the guidelines of the Institutional Committee of Ethic at Faculty of Dentistry, Tanta University.

Chemicals and reagents

Alloxan monohydrate was obtained from Sigma-Aldrich (St Louis, MO, USA). Ozone was generated with ozonator equipment (Ozone Longevity Resources Dwyermade, Canada). The ozone concentration in the O3/O2 mixture was 50 µg/ml and was i.p. administered. Ozone was attained from medical grade oxygen and was used immediately upon generation and represented only about 3% of the O3/O2 gas mixture. The ozone concentration was measured using a UV spectrophotometer at 254 nm. The ozone administrated to each animal and regulated to a final dose of 1.1 mg/kg BW (12).

Induction of Diabetes mellitus

Diabetes was induced by a single intraperitoneal administration of alloxan (140mg/kg) with 4% saline solution (an average of 0.90 mL per specimen) (13). Before administering alloxan, we acquired a baseline glycemia. After twelve hours blood were sampled from the tail vein of each rat. After five days the rats displayed levels above 300mg/dL were considered diabetic.

Experimental design

Thirty male albino rats were used and randomly divided into 3 groups as follows; group I (control group): ten rats injected intraperitoneal (i.p.) citrate buffer (0.1 M, pH 4.5), group II (diabetic group): ten rats received single (i.p.) administration of alloxan (140mg/kg) with 4% saline solution (an average of 0.90 mL per specimen), group III (ozone group): ten diabetic rats received (i.p.) administration of ozone at a dose of 1.1 mg/kg. This dose of ozone has been shown to manage oxidative condition without toxicity (14).

Animal sacrifice

The rats from each group were euthanized 6 weeks after experiment using overdose of anesthesia. SMGs were removed.

Histological examination

Right SMGs were removed and fixed in a 10% formaldehyde solution for 12 hours, washed by tap water, dehydrated in ascending grades of ethyl alcohol, cleaned in xylol and embedded in paraffin wax. Sections of 5 µm mounted on clean glass slides and stained with Haematoxylin and Eosin stain for light microscopic examination.

Transmission electron microscopic examination

Left SMGs. Samples were cut into small pieces and fixed for 2 h with a mixture of 1% paraformaldehyde and 1.25% glutaraldehyde in 0.1 M cacodylate buffer (pH 7.2). Then, they were rinsed in cacodylate buffer supplementary with 3.5% sucrose, fixed with osmium tetroxide, dehydrated, and embedded in Epon Resin. Semi thin sections stained with toluidine blue were observed. Ultrathin sections (90– 100 nm) were cut with a diamond knife, collected on grids, stained with uranyl acetate and bismuth subnitrate, and finally observed and photographed in a JEOL 100S (Faculty of medicine, Tanta University).

3. Results

Light Microscopic Histological Examination

Hematoxylin and eosin stained sections of the rat SMG in control group revealed the normal architecture of the glandular tissue. It showed normal serous, mucous and mixed acini with striated ducts. The serous and mucousacini were lined with pyramidal cells with large rounded basal nuclei and flat basal nuclei respectively, their cytoplasm was appeared basophilic. Striated ducts were lined with single layer of columnar cells with acidophilic cytoplasm. The intercalated ducts were lined by small cuboidal cells having central rounded nuclei. Granular convoluted tubules (GCT) in between acini were lined with columnar cells and packed with intensely stained eosinophilic granules. The excretory ducts were lined with pseudo stratified columnar epithelium with goblet cells, appeared in C.T septa between lobes and

lobules. All these parenchymal elements were embedded in reticular CT stroma (Fig. 1).

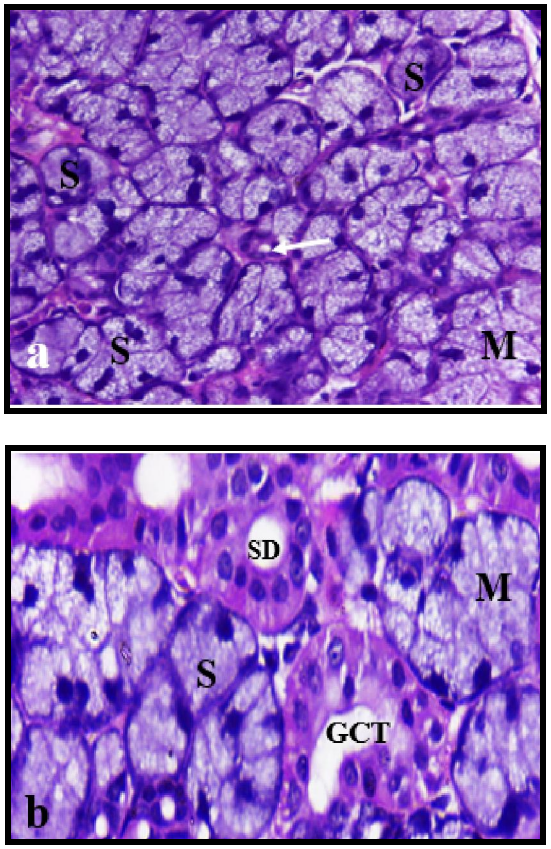

Fig. (1): A photomicrograph of rat SMG of control group (group I) showing: (**a**) normal architecture of the glandular tissue, Serous acini (S), and mucous acini (M), intercalated ducts in between acini (white arrows). (**b**) Higher magnification of serous acini (S), and mucous acini (M) with striated duct (SD), granular convoluted tubules (GCT) (H & E a X 200 and b X 400).

Hematoxylin and eosin stained sections of the rat SMG in diabetic group showed sever degenerative changes of the glandular tissue. The acini showed intracytoplasmic vacuolization with displacement of the nuclei. The nuclei of the acinar cells revealed different sizes, shape. Atrophic striated ducts with loss of cell arrangement were noticed with many cytoplasmic vacuoles and narrow lumen. the degenerated ducts were appeared surround by congested blood capillaries. GCT demonstrated degenerative changes manifested as loss of structural integrity, wide lumen with retained eosinophilic secretory material (Fig. 2).

Hematoxylin and eosin stained sections of the rat SMG in ozone group showed little destructive changes. Reversion of the destructive effects of diabetes on SMG was noticed and SMG nearly exhibited a normal architecture pattern. Normal acini structure with small number of intracytoplasmic vacuolization were appeared. The nuclei of the acinar cells revealed limited changes in size and shape. The striated ducts reveled normal arrangement of their cells with small number of cytoplasmic vacuoles and normal lumen. GCT demonstrated little degenerative changes manifested as nearly normal lumen with little amount of eosinophilic secretory material and a degree of loss of cells integrity. The excretory ducts showed small number of cytoplasmic vacuoles. Dilated congested blood capillaries noticed around striated ducts and excretory ducts (Fig. 3).

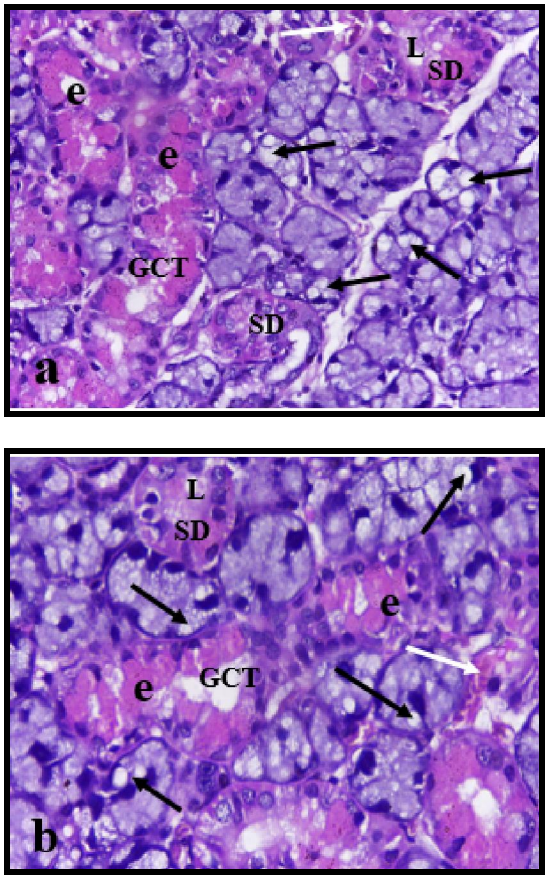

Fig. (2): A photomicrograph of rat SMG of diabetic group (group II) showing: (**a**) (**b**) Degenerative changes of the glandular tissue, the acini showed intracytoplasmic vacuolization (black arrows), atrophic striated duct (SD) with loss of cell arrangement and narrow lumen (L). granular convoluted tubules (GCT) with loss of structural integrity wide lumen with retained eosinophilic secretory material (e). Congested blood capillaries (white arrows). (H & E **a** X 100 and **b** X 200).

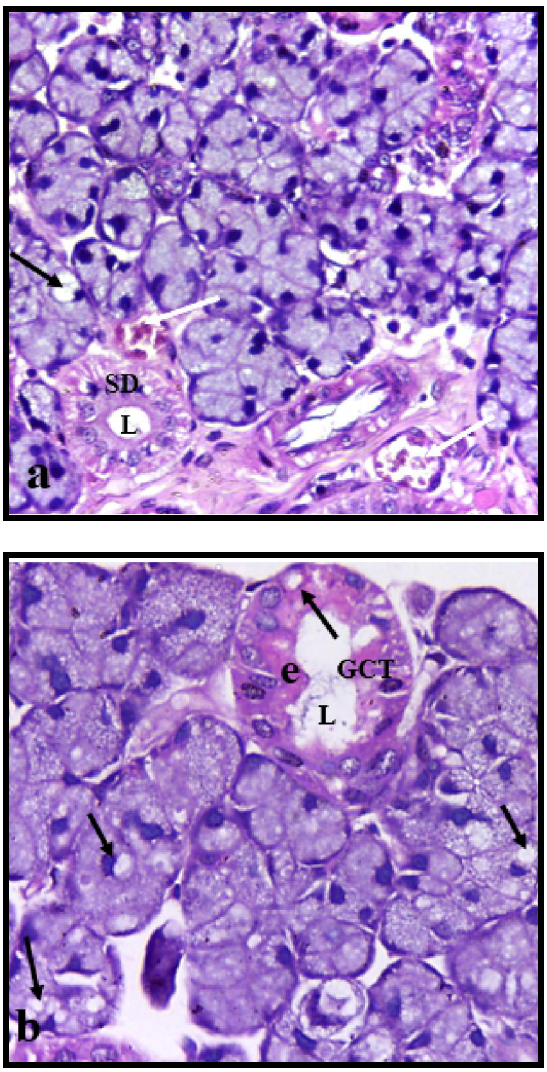

Fig. (3): A photomicrograph of rat SMG of ozone group (group III) showing: (**a**) (**b**) Little destructive changes with almost restoring the normal architecture of the glandular tissue, normal acini structure with small number of intracytoplasmic vacuolization (black arrows), striated duct (SD) showed normal arrangement of their cells with small number of cytoplasmicvacuoles (black arrows) and normal lumen (L). Granular convoluted tubules (GCT) demonstrated little degenerative changes, nearly normal lumen (L) with little amount of eosinophilic secretory material (e). Dilated congested blood capillaries (white arrows). (H & E **a** X 200 and **b** X 400).

Electron Microscopic Examination

The ultrastructure of the rat SMG in control group showed glandular acini with large pyramidal cells. Rounded nucleus and prominent nucleolus for serous acinar cell were recorded. While, it was appeared as flat nucleus for mucous acinar cell. Their chromatin was arranged adjacent to the inner nuclear membrane in aggregated form and the rest of chromatin was dispersed in the matrix of the nucleus forming an open-faced nucleus. Regularly packed parallel arrays of rough endoplasmic reticula (RER) and mitochondria were seen in their cytoplasm. Mature secretory electron dense vesicles were appeared as homogenous variable sized founded on the apical portion of the serous acinar cell, while it was appeared as electron lucent secretory granules for the mucous acinar cell. Striated duct appeared lined by tall columnar cells with open faced nucleus, basal infoldings filled with mitochondria, and prominent desmosomal junctions. Myoepithelial cells possessing many long processes intervening between the basement membrane and basal surface of acinar cells and intercalated duct (Fig. 4,5).

The ultrastructure of the rat SMG in diabetic group showed serous acinar cells with irregular dark nuclei with clumped chromatin and perinuclear spaces, depletion of secretory vesicles. Large cytoplasm vacuoles with some swollen mitochondria and others degenerated with irregular cristae were appeared. Irregular degenerated and dilated RER were scattered in the cytoplasm. The mucous acinar cells showed shrunk nucleus, other nuclei irregular in shape, and other were pyknotic. This cell characterized by presence of large electron lucent secretory vesicles, some of these vesicles were coalescing together, irregular dilated degenerated RER were scattered in the cell. The striated duct showed signs of sever degenerative changes. The nuclei appeared with different sizes and shapes and some were pyknotic and other were dark stained. Decrease in basal infoldings of the basal plasma membrane were noticed in addition to degenerated mitochondria and mega mitochondria, and large intracytoplasmic vacuolization. Other ductal cells revealed cytoplasmic rarefaction with phagosomes engulfing mitochondria and RER. Myoepithelial cell showed clumping of the nuclear chromatin with disorganized basal lamina (Fig. 6,7,8).

The ultrastructure of the rat SMG in ozone group showed serous acinar cells with normal nuclei others with small nuclei, secretory electron dense vesicles were appeared as homogenous variable sized. Small cytoplasm vacuoles with regularly packed parallel arrays of RER which showing little amount of dilatation. The mucous acinar cells showed normal flat nucleus, electron lucent secretory vesicles, regularly packed parallel arrays of RER were scattered in the cell. The striated duct showed very little signs of degenerative changes. The nuclei appeared with open faced nucleus some nuclei were small. Basal infoldings filled with mitochondria were noticed in addition to small number of degenerated mitochondria, and intracytoplasmic vacuolization. Myoepithelial

possessing long processes intervening between the basement membrane and basal surface of acinar cells, some cells appeared with normal nucleus others showed little amount of nuclear clumping chromatin (Fig. 9,10,11).

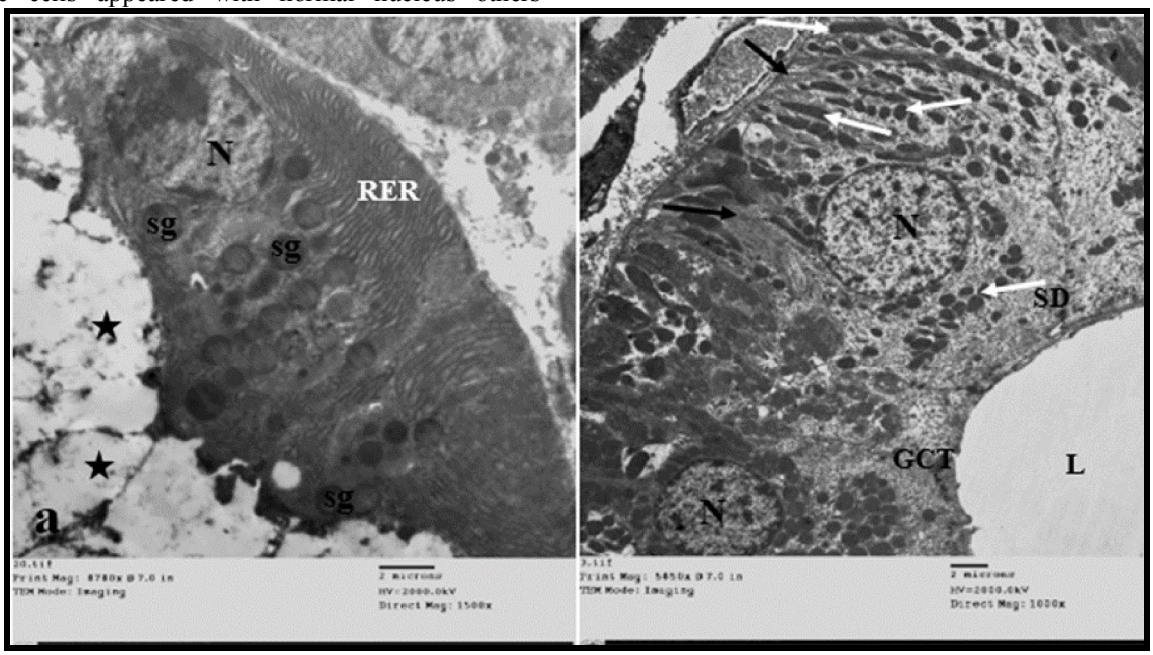

Fig. (4): Electron photomicrographs of rat SMG of group I (control group) showing: (**a**) Part of the secretory portion having serous acinar cells with large open face nucleus (N), packed parallel arrays of RER and electron dense secretory granules (sg). (**b**) Line border between striated duct cells (SD) & granular convoluted tubules (GCT), tall columnar cells of SD, open faced nucleus (N), basal infoldings (black arrows) filled with mitochondria (white arrows), prominent desmosomal junctions (arrow head). Mucous secretory granules (star), lumen (L) (A TEM x 1500and B TEM x 1000).

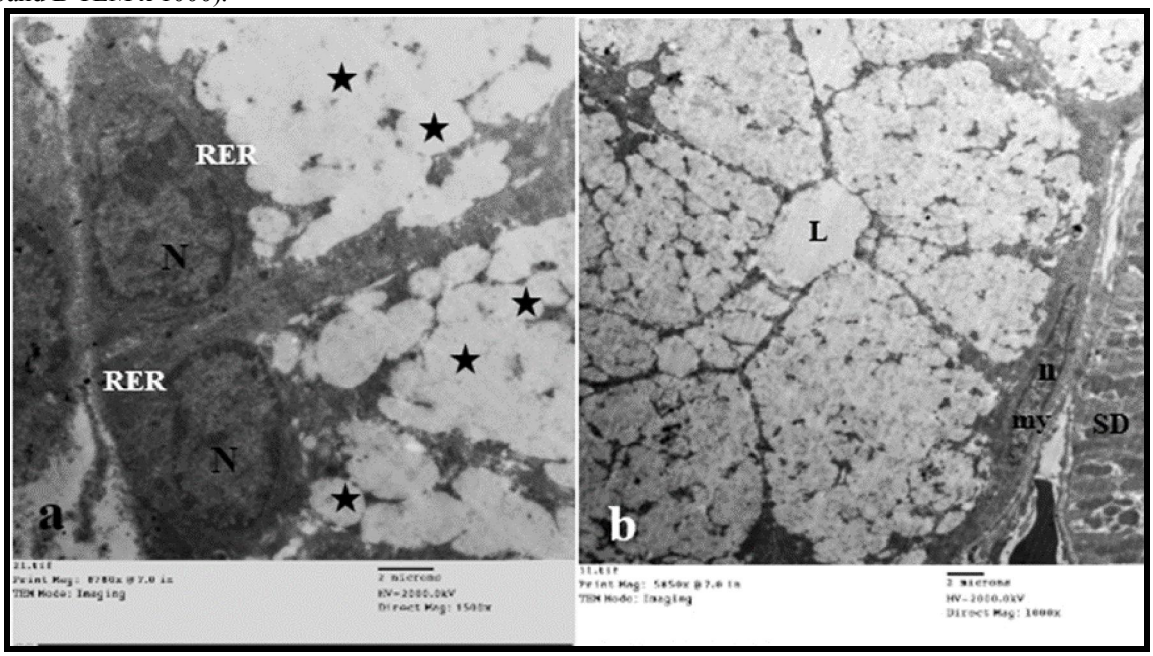

Fig. (5): Electron photomicrographs of rat SMG of group I (control group) showing: (**a**) Part of the secretory portion having mucous acinar cells with large flat nucleus (N), parallel arrays of RER and electron lucent secretory granules (star). (**b**) mucous acini with large pyramidal cells filled with secretory granules surrounding large lumen (L). Myoepithelial cell (my) with dispersed nucleus chromatin (n), it is intervening between the basement membrane and basal surface of acinar cells. striated duct cells (SD) (A TEM x 1500and B TEM x 1000).

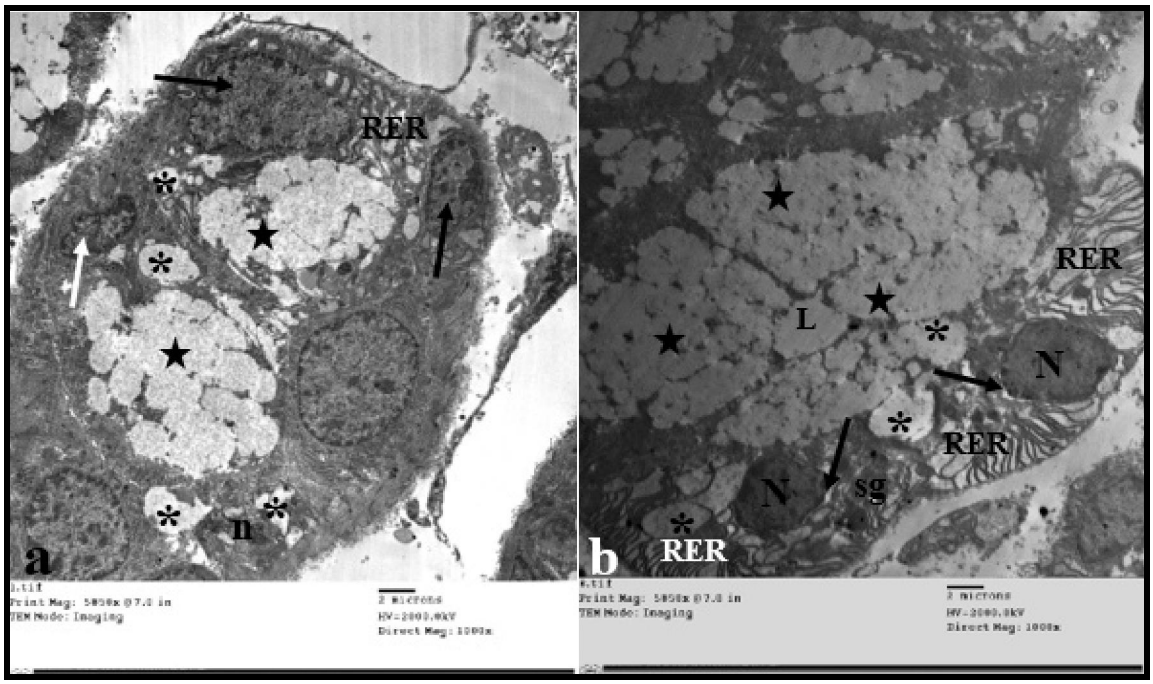

Fig. (6): Electron photomicrographs of rat SMG of group II (diabetic group) showing: (**a**) Part of the secretory portion having mucous acinar cells with shrunk nuclei (white arrows), irregular shape nuclei (black arrows), and pyknotic nuclei (n). coalescing of mucous secretory granules (star). Irregular degenerated and dilated RER. (**b**) Part of the secretory portion having serous acinar cells with irregular dark nuclei with clumped chromatin (N) and perinuclear spaces (black arrows), depletion of secretory vesicles (SG). Large cytoplasm vacuoles (asterisk), irregular degenerated and dilated RER. lumen (L) (A and B TEM x 1000).

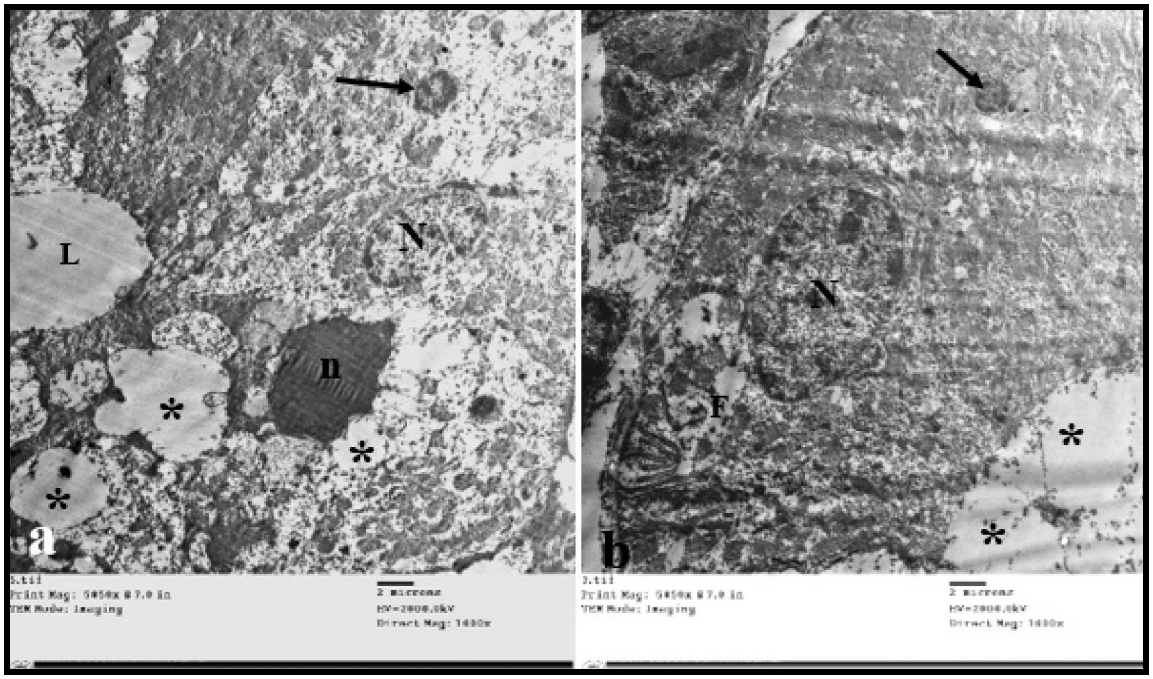

Fig. (7): Electron photomicrographs of rat SMG of group II (diabetic group) showing: (**a**) & (**b**) Striated duct cells showed signs of sever degenerative changes, pyknotic nuclei (black arrows), dark stained nuclei (n), large intracytoplasmic vacuolization (asterisk), and phagosomes engulfing mitochondria and RER (F). open faced nucleus (N) (A TEM x 1000and B TEM x 1500).

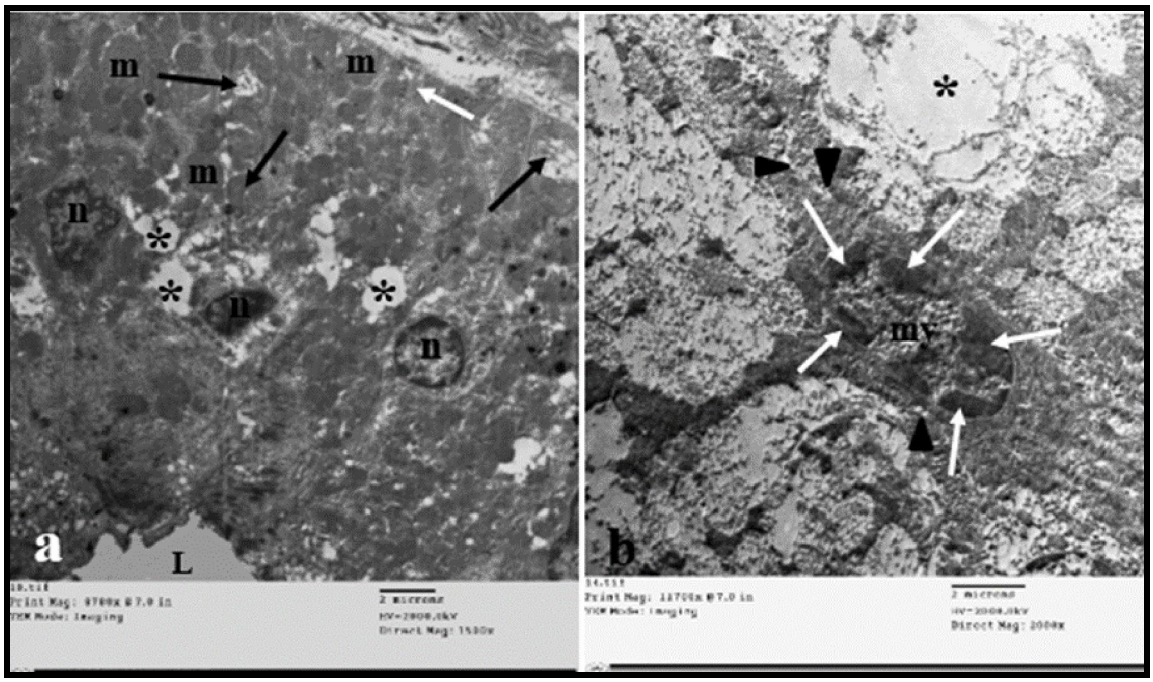

Fig. (8): Electron photomicrographs of rat SMG of group II (diabetic group) showing: (**a**) Striated duct cells showed pyknotic nuclei (n), Decrease or degeneration of basal infoldings (white arrows), degenerated mitochondria (black arrows), mega mitochondria (m) and intracytoplasmic vacuolization (asterisk). (**b**) Myoepithelial cell (my) showed clumping of the nuclear chromatin (white arrows) with disorganized basal lamina (black arrows heads). SD lumen (L) (A TEM x 1500and B TEM x 2000).

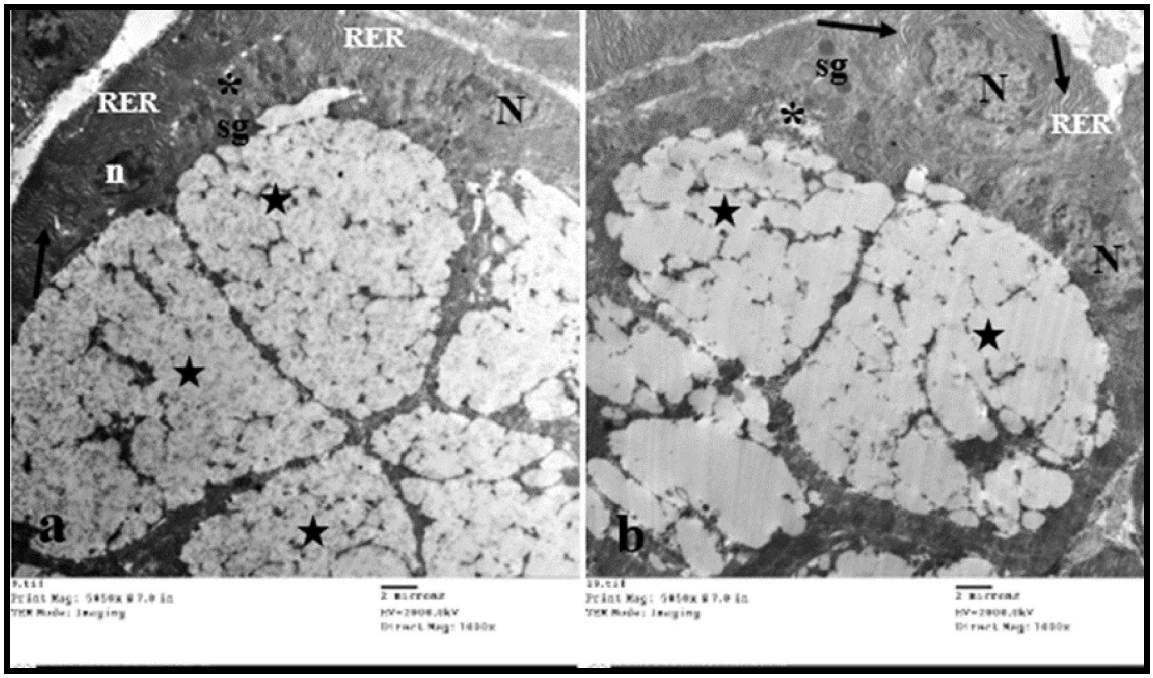

Fig. (9): Electron photomicrographs of rat SMG of group III (ozone group) showing: (**a**) & (**b**) Part of the secretory portion having serous acinar cells with large open face nucleus (N), small nucleus (n), packed parallel arrays of RER some showing little amount of dilatation (black arrows) and electron dense secretory granules (sg). Small cytoplasm vacuoles were appeared (asterisk). Mucous secretory granules (star) (A and B TEM x 1000).

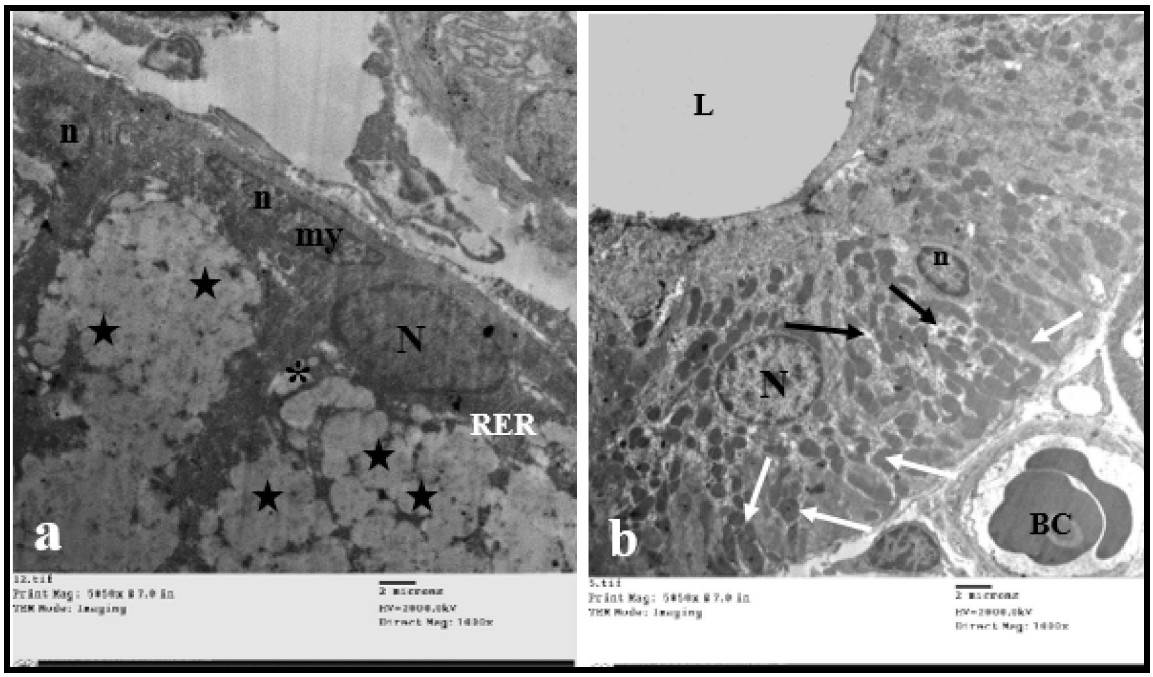

Fig. (10): Electron photomicrographs of rat SMG of group III (ozone group) showing: (**a**) Part of the secretory portion having mucous acinar cells with large flat nucleus (N), other showing small nucleus (n), parallel arrays of RER and electron lucent mucous secretory granules (star), small cytoplasm vacuoles were appeared (asterisk). Myoepithelial cell (my) with dispersed nucleus chromatin (n), it is intervening between the basement membrane and basal surface of acinar cells. (**b**) Tall columnar cells of striated duct cells SD, open faced nucleus (N), small nucleus (n), basal infoldings filled with mitochondria (white arrows), little intracytoplasmic vacuolization (black arrows). SD lumen (L), blood capillary (BC) (A and B TEM x 1000).

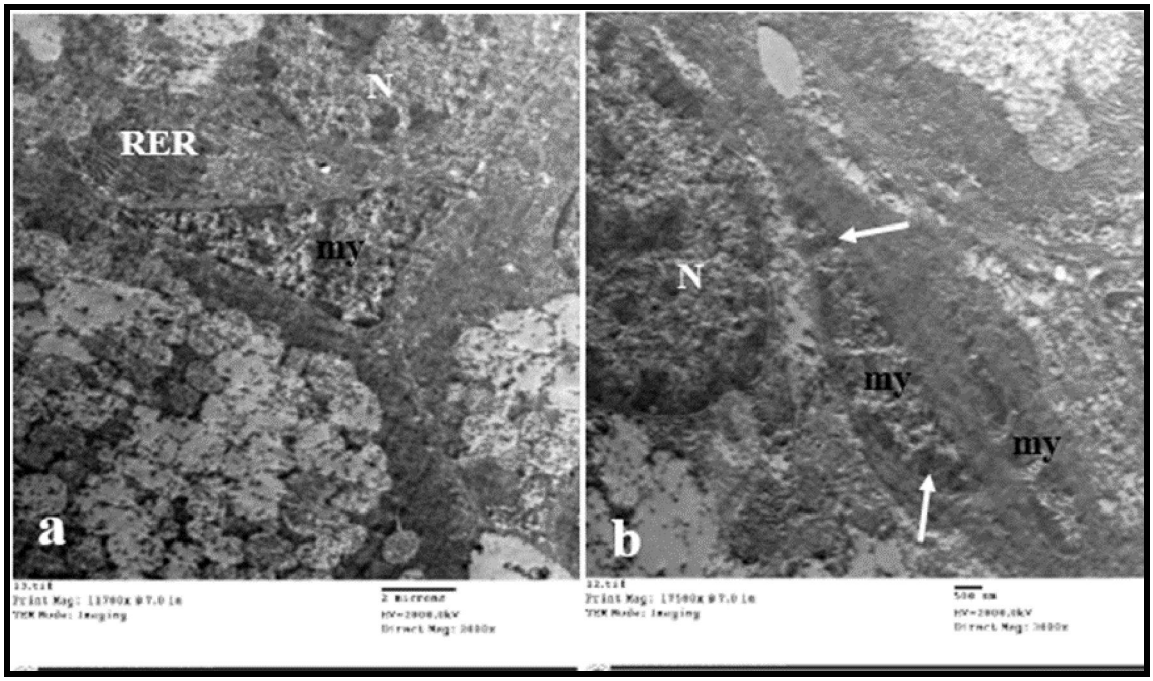

Fig. (11): Electron photomicrographs of rat SMG of group III (ozone group) showing: (**a**) Myoepithelial cell (my) with dispersed nucleus chromatin, it is intervening between the basement membrane and basal surface of acinar cells. (**b**) Myoepithelial cell (my) showed little amount of clumping nuclear chromatin (white arrows), nucleus of secretory cell (N), parallel arrays of RER (A TEM x 2000and B TEM x 3000).

4. Discussion

DM is a metabolic disease that is characterized by hyperglycemia resulting from insufficiency and /or dysfunction of insulin (15). The state of chronic hyperglycemia of diabetes mellitus is usually associated with long term damage, dysfunction and failure of different organs in the body leading to different numerous complications(16).

The SMG is one of the three major salivary glands and is of interest in many different fields of biological research(17). A variety of pathological changes in acini of SMG were demonstrated in diabetes (18). It was suggested that diabetic changes in salivary glands were attributed to accumulation of oxidative stresses within the glands(19).

Ozone is composed of three oxygen atoms that was found to prevent oxidative stress in diabetic rats(20). In addition, ozone treatment was shown to reduce hyperglycemia and decrease damaged pancreatic islets (21). Therefore, it seems that ozone may be a potential therapeutic target to reduce damaging effects of diabetes on SMG.

In the present study, we evaluated the effect of ozone treatment on the regeneration of SMG in diabetic rats. Diabetes was induced in rats by alloxan. Administration of alloxan in rodents and many other animal species provokes degeneration of beta cells of pancreas in a manner mimicking type-1 DM in human (22). Destruction of beta cells was shown to be partially mediated by free radicals as reactive oxygen species (ROS) (23).

In diabetic group, light microscopic and ultrastructural appearance of SMG revealed destructive changes. Electron microscope showed that some of the nuclei exhibited variation in size, pyknosis and dark staining in both acini and striated ducts. In addition, degenerated swollen mitochondria, irregular dilated RER with many cytoplasmic vacuoles are also detected. Myoepithelial cells revealed chromatin clumping and disorganized basal lamina in some cells. These ultrastructural findings are consistent with other previous reports in experimental diabetes in which salivary gland tissue exhibited destructive changes in acinar and ductal segments (24, 25). The destructive effect of hyperglycemia seen in this group may contribute to induction of oxidative stresses (19). Several mechanisms may be involved in this process and include glucose autoxidation and activation of polyol pathway that was shown to be implicated in diabetic complications (26). In addition, elevated free fatty acids in diabetes may have a role in increasing ROS generation (27). Moreover, it was demonstrated that cellular injury caused by oxidative stresses may be enhanced by DNA fragmentation and membrane peroxidation (28).

In the current study, better microscopical changes in SMG were observed in ozone treated diabetic rats and ozone almost restored the normal structure of the gland after six weeks. It has been reported that ozone therapy induced production of 2,3 diphosphoglycerate causing an elevation in the amount of oxygen released to tissues (20) Moreover, it has been recognized that ozone can reduce hyperglycemic state as ozone had anti-diabetic effect (21). Because ozone is a rapid and strong oxidizing agent, it has been suggested that it can be able to induce an antioxidant effect that may result in modulating the condition of oxidative stress that is responsible for destructive effects of diabetes(29).

Furthermore, it was seen that ozone immediately dissolved in the water overlying the epithelium after intraperitoneal injection producing hydrogen peroxide which may influence cellular metabolisms and thus facilitates tissue regeneration (30). It has been reported that ozone therapy stimulates the production of prostacyclin and enzymes that can act as free radical scavengers and cell wall protectors (31). Moreover, it increases the production of tumor necrosis factor, interleukin-2 and interferon enhancing the immune system (32).

Based on the results of this work, we can conclude that ozone is a potent oxidizer that might be essential for modifying the condition of oxidative stress associated with diabetes. Moreover, it can partially improve and reverse the damaging effects and cellular changes observed in SMGs in experimental diabetes within the limited period of this study. Therefore, our findings highlight the potential role of ozone as an effective.

Reference

1. Norris SL, Zhang X, Avenell A, Gregg E, Schmid CH, Lau JJCDo SR. Pharmacotherapy for weight loss in adults with type 2 diabetes mellitus. 2005(1).
2. Guzmán JR, Lyra R, Aguilar-Salinas CA, Cavalcanti S, Escaño F, Tambasia M, et al. Treatment of type 2 diabetes in Latin America: a consensus statement by the medical associations of 17 Latin American countries. 2010;28:463-71.
3. Akpan H, Adefule A, Fakoya F, Caxton-Martins EJJAS. Evaluation of LDH and G6-PDH activities in auditory relay centers of streptozocin-induced diabetic wistar rats. 2007;1(1):21-5.
4. Löe HJDc. Periodontal disease: the sixth complication of diabetes mellitus. 1993;16(1):329-34.
5. Al-Faris NA, Al-sawadi AD, Alokail MSJSjobs. Effect of samh seeds supplementation (Mesembryanthemum forsskalei Hochst) on liver

enzymes and lipid profiles of streptozotocin (STZ)-induced diabetic Wistar rats. 2010;17(1):23-8.
6. Öngöz Dede F, Bozkurt Doğan Ş, Balli U, Avci B, Durmuşlar M, Baratzade TJJopr. Glutathione levels in plasma, saliva and gingival crevicular fluid after periodontal therapy in obese and normal weight individuals. 2016;51(6):726-34.
7. Russotto SBJOs, oral medicine, oral pathology. Asymptomatic parotid gland enlargement in diabetes mellitus. 1981;52(6):594-8.
8. Lindeberg H, Andersen LJAoo-r-l. The size and composition of the submandibular glands in late-onset diabetes. 1987;244(2):100-3.
9. Bocci VAJAomr. Tropospheric ozone toxicity vs. usefulness of ozone therapy. 2007;38(2):265-7.
10. Morsy MD, Hassan WN, Zalat SIJD, Syndrome M. Improvement of renal oxidative stress markers after ozone administration in diabetic nephropathy in rats. 2010;2(1):29.
11. Martínez-Sánchez G, Al-Dalain SM, Menéndez S, Re L, Giuliani A, Candelario-Jalil E, et al. Therapeutic efficacy of ozone in patients with diabetic foot. 2005;523(1-3):151-61.
12. Kumar S, Kumar D, Deshmukh R, Lokhande P, More S, Rangari VJF. Antidiabetic potential of Phyllanthus reticulatus in alloxan-induced diabetic mice. 2008;79(1):21-3.
13. Peralta C, Xaus C, Bartrons R, Leon OS, Gelpí E, Roselló-Catafau JJFrr. Effect of ozone treatment on reactive oxygen species and adenosine production during hepatic ischemia-reperfusion. 2000;33(5):595-605.
14. Barber E, Menéndez S, León O, Barber M, Merino N, Calunga J, et al. Prevention of renal injury after induction of ozone tolerance in rats submitted to warm ischaemia. 1999;8(1):37-41.
15. care ADAJD. Diagnosis and classification of diabetes mellitus. 2013;36(Supplement 1):S67-S74.
16. Kitabchi AE, Umpierrez GE, Miles JM, Fisher JNJDc. Hyperglycemic crises in adult patients with diabetes. 2009;32(7):1335-43.
17. Amerongen AN, Veerman EJOd. Saliva–the defender of the oral cavity. 2002;8(1):12-22.
18. High A, Sutton J, Hopper AJAoob. A morphometric study of submandibular salivary gland changes in streptozotocin-induced diabetic rats. 1985;30(9):667-71.
19. Knaś M, Maciejczyk M, Daniszewska I, Klimiuk A, Matczuk J, Kołodziej U, et al. Oxidative damage to the salivary glands of rats with streptozotocin-induced diabetes-temporal study: oxidative stress and diabetic salivary glands. 2016;2016.
20. Al-Dalain SM, Martínez G, Candelario-Jalil E, Menéndez S, Re L, Giuliani A, et al. Ozone treatment reduces markers of oxidative and endothelial damage in an experimental diabetes model in rats. 2001;44(5):391-6.
21. Martinez G, Al-Dalain SM, Menendez S, Guiliani A, Leon OSJAFB. Ozone treatment reduces blood oxidative stress and pancreas damage in a streptozotocin-induced diabetes model in rats. 2005;24(4):491.
22. Szkudelski TJPr. The mechanism of alloxan and streptozotocin action in B cells of the rat pancreas. 2001;50(6):537-46.
23. Ekuni D, Endo Y, Irie K, Azuma T, Tamaki N, Tomofuji T, et al. Imbalance of oxidative/anti-oxidative status induced by periodontitis is involved in apoptosis of rat submandibular glands. 2010;55(2):170-6.
24. Anderson LCJBR. Salivary gland structure and function in experimental diabetes mellitus. 1998;9:107-19.
25. El Sadik A, Mohamed E, El Zainy AJPo. Postnatal changes in the development of rat submandibular glands in offspring of diabetic mothers: Biochemical, histological and ultrastructural study. 2018;13(10):e0205372.
26. Jay D, Hitomi H, Griendling KKJFRB, Medicine. Oxidative stress and diabetic cardiovascular complications. 2006;40(2):183-92.
27. Murphy MPJBj. How mitochondria produce reactive oxygen species. 2009;417(1):1-13.
28. Pizzimenti S, Toaldo C, Pettazzoni P, Dianzani MU, Barrera GJC. The" two-faced" effects of reactive oxygen species and the lipid peroxidation product 4-hydroxynonenal in the hallmarks of cancer. 2010;2(2):338-63.
29. He Q, Krone K, Scherl D, Kotler M, Tavakkol AJSp, physiology. The use of ozone as an oxidizing agent to evaluate antioxidant activities of natural substrates. 2004;17(4):183-9.
30. Bocci V. Ossigeno-ozonoterapia. Casa Editrice Ambrosiana. Milano, 1-324.
31. Elvis A, Ekta JJJons, biology, medicine. Ozone therapy: A clinical review. 2011;2(1):66.
32. Bocci V. The clinical application of ozone therapy. In: Ozone BA, editor. A New Medical Drug. Amsterdam, The Netherlands: Springer; 2005. p. 97–226.